Preparation and Characterization of a Nanoparticles Modified Chitosan Sensor and Its Application for the Determination of Heavy Metals from Different Aqueous Media

Rasha A. Ahmed[1,2,*]*, A.M. Fekry*[3]

[1]Kingdom of Saudi Arabia, Taif University, Faculty of science, Chemistry dept.
[2]Forensic Chemistry Laboratories, Medico Legal Department, Ministry of Justice, Cairo, Egypt.
[3] Chemistry Department, Faculty of Science, Cairo University, Giza 12613, Egypt.
[*]E-mail: Rashaauf@yahoo.com

A biosensor electrode based on the incorporation of super nanoparticles paramagnetic iron oxide (α-Fe_3O_4) in chitosan (CS) film coated on platinum electrode, was developed for the determination and removal of heavy metals. The morphological properties of the homogenous α-Fe_3O_4/CS nanocomposite were studied with scanning electron microscopy (SEM), Energy Dispersive X-ray analysis (EDX), and thermal gravimetric analysis (TGA). The morphological results indicate the successful formation of α-Fe_3O_4/CS nanocomposite and high stability of the film. The α-Fe_3O_4/CS nanocomposite showed a great efficiency for the determination of As, Pb, and Ni ions from aqueous solution using various electrochemical techniques. The presence of α-Fe_3O_4 nanoparticles results in increased active surface area and enhanced electron transfer. Results showed that this novel α-Fe_3O_4/CS nanocomposite was successfully applied for sewage water and human urine samples with very low detection limit.

1. INTRODUCTION

Heavy metals are elements that are naturally found in the earth's crust. They can be introduced in environment as a consequence of human activities and rapid industrialization. Trace amounts of heavy metals are essential to the human body, however, high concentrations can be dangerous leading to a damage of human health, due to they are non-biodegradable and can be accumulated in living tissues. Therefore, determination of trace levels of heavy metals is very critical for environmental protection, food and agricultural chemistry and also for monitoring environmental pollution [1–3].

Lead (Pb), is a non-physiological metal and environmental pollutant that is exposed to most of the general human population below levels known to cause clinical effects of toxicity. It has been demonstrated to be accumulated in bone and in some soft tissues, such as liver, kidney and brain. Toxic effects of Pb are manifested in the central nervous system, where encephalopathy, seizures and irritability are the most severe symptoms observed [4, 5]. Although, Nickel (Ni) is an essential nutrient for plants; in which they need a very low concentration of it for a normal growth, but it is a toxic metal and a known carcinogen. It mainly results from effluent disposal from mining, smelting and electroplating industries, and from sewage sludge and compost [6-12]. Soil and water contamination with Ni has become a worldwide problem [13, 14]. Arsenic (As) is released into air by volcanoes. It is also a natural contaminant of some deep-water wells that occurs in many minerals, usually in conjunction with sulfur and metal. Additionally, Arsenic and many of its compounds are especially potent poisons, causing arsenicosis owing to its manifestation in drinking water. Many water supplies close to mines are contaminated by these poisons [15].

For the removal of heavy metals from aqueous solution electrochemical precipitation, ion exchange, ultrafiltration, and reverse osmosis [16-22] are used. Electrochemical techniques are preferred for the in situ measurements of Heavy metals due to their high sensitivity, good selectivity, low cost, simplicity, and easy data read-out [23–30]. Among of them, cyclic voltammetry (CV), impedance and anodic stripping linear sweep voltammetry (ASLSV) provide a powerful tool for metal ions determination [31, 32].

The metal adsorption capacity of several low-cost adsorbents, such as biopolymers, has been investigated in the present study. These biopolymers, which are obtained from renewable sources, can selectively adsorb several metallic ions [33]. Chitosan (CS) is one of them that have proved to be an extremely promising material. It is a natural biopolymer produced by the alkaline N-deacetylation of chitin, the most abundant after cellulose [34–39]. Chemical modifications of CS may include chemical cross-linking (to increase polymer stability in acidic solutions) or grafting of new functional groups (to increase the adsorption sites), which can increase the adsorption capacity and selectivity toward the metal ions in the solution [40–43]. Crosslinking agents like Glyoxal (GO), Epichlorohydrin (ECH), Glutaraldehyde (GA), and 1-Ethyl-3-(3-dimethylaminopropyl) carbodiimide together with N-hydroxysuccinimide (EDC-NHS) are examples of chemical modifications on CS [44].

Metal oxide nanoparticles such as Fe_3O_4 [45–47], ZnO [48, 49], CeO_2 [50, 51] etc. have been suggested as promising matrices and they exhibit large surface-to-volume ratio, high surface reaction activity, high catalytic efficiency and strong adsorption ability that can be helpful to obtain improved stability and sensitivity of a biosensor. Moreover, they have a unique ability to promote fast electron transfer between electrode and the active site of an enzyme. Among of them, Fe_3O_4 nanoparticles, which are of special interest due to its biocompatibility, strong super paramagnetic behavior and low toxicity. Since magnetic behavior of these bioconjugates may result in improved delivery and recovery of molecules. Besides this, existing problem of aggregation and rapid biodegradation of Fe_3O_4 nanoparticles onto a given matrix can perhaps be overcome by modifying these nanoparticles using CS by preparing nanocomposite [52–59]. CS displays an excellent film-forming ability, good adhesion, biocompatibility, high mechanical strength and susceptibility to chemical modification due to the presence of reactive hydroxyl and amino functional groups. Efforts have recently been made to

improve optical and electrical properties of CS for biosensor application by dispersing super paramagnetic Fe_3O_4 nanoparticles [52, 59]. Both Metal oxide nanoparticles and chitosan can remove heavy metals from aqueous environments, but, to the authors' knowledge, there are no studies exploring the potentiality of combining these two adsorbents in the form of a composite and using it for heavy metal removal from aqueous solution. In this study, a novel nanocomposite made of α-Fe_3O_4 and CS was prepared. The α-Fe_3O_4/CS nanocomposite was characterized using various techniques to verify the modification, and the nanocomposite modified electrode was used for the determination and removal of Arsenic, Lead, and Nickel ions from aqueous solution.

2. EXPERIMENTAL

2.1. Reagents and Solutions preparation

Chitosan (degree of deacetylation 85% and Mw 1.0×10^5 Da), α- Fe_3O_4 nanoparticles and As(III), Pb(II), Ni(II) were purchased from Sigma Aldrich. Glutaraldehyde, Nitric acid and all the other reagents used in this experiment were of analytical grade and used as received without further purification. Double distilled water (DDW) was used throughout the experiments. A stock solution of Ni(II), As(III) and Pb(II) (5.0×10^{-3} M) was prepared using double distilled water. It was later diluted to desired concentrations using 0.05 mol L^{-1} KNO_3 and pH adjusted with 0.05 mol L^{-1} KOH.

2.2. Preparation of α-Fe₃O₄/CS nanocomposite

α-Fe_3O_4 nanoparticles are dispersed into 10 mL of CS (0.3 mg/mL) solution in acetic acid under continuous stirring at room temperature after which it is sonicated for about 4 h. Finally, viscous red solution of CS with uniformly dispersed α-Fe_3O_4 nanoparticles is obtained. 10 μL of α-Fe_3O_4/CS nanocomposite films have been fabricated uniformly by spin coating process onto Pt electrode surface (surface area is $0.07cm^2$) and allowing it to dry at room temperature for 1 h. The nanocomposite films are washed repeatedly with distilled water to remove any unbound particles.

A smooth and red transparent layer, covering the Pt surface, was visually observed. The α-Fe_3O_4/CS nanocomposite films are then dipped in 10 μL of 2.0% (v/v) of cross linker glutaraldehyde solution for 1 min, and left to dry for 24 hours before use.

2.3. Instrumentation

The measurements were carried out with a potentiostat/galvanostat instrument. EIS measurements were done using Autolab PGSTAT 73022 at an open circuit potential with applied 10 mV sinusoidal perturbations in the 100 kHz to 0.1 mHz frequency range, taking 7 steps per decade was used. For this purpose, a conventional three-electrode cell was used, composed of calomel reference electrode, a platinum wire as the counter electrode, and the α-Fe_3O_4/CS nanocomposite modified platinum as the working electrodes. All the measurements were done in a Faraday cage in order to

avoid electromagnetic interference and the impedance plots were fitted using FRA software. The voltammetric measurements were scanned from -2.0 V to 2.0 V with a scan rate of 50 mV s^{-1}.

Scanning electron microscopy (SEM) (Philips, XI 30) was used for characterization of the homogeneity of the coatings; the samples were coated with gold before SEM examination.

Thermogravimetric analysis (TGA) was done using TGA-50H Shimadzu thermogravimetric analyzer. Samples were heated from 0 to 500 ^{o}C in a platinum pan with a heating rate 10 ^{o}C/min, in N$_2$ atmosphere of flow rate 25 mL/min.

Elemental film composition was analyzed using FEI Quanta FEG microscope equipped with Oxford Link EDX microanalysis hardware.

2.4. Analytical procedure

The metals determination with the modified electrode was evaluated by linear sweep voltammetry (LSV). The experimental conditions were 0.05 mol L^{-1} KNO$_3$ solution using an accumulation potential of -0.6 V applied for 600 s, in a potential range from -2.0 to 2.0 V vs. calomel reference electrode raised at a scan rate of 50 mV s^{-1}. The standard addition method was applied for Ni(II), As(III) and Pb(II) determination in real samples of sewage water and human urine using the proposed modified electrodes. Then, small volumes of a standard Ni(II), As(III) and Pb(II) solution were added and the respective voltammograms were recorded.

The recovery studies were realized with a solution with well known concentration and considered true and the percentage recovery was calculated. Various known amounts of Ni(II) were added to the samples and were subsequently analyzed by proposed electrode.

3. RESULTS AND DISCUSSION

3.1. Comparative and Characterization of the composite films.

The physical characterization of the nanocomposite is crucial to prove that the nanomaterials were well incorporated in the chitosan film. Different techniques were used to study and validate the structure of α-Fe$_3$O$_4$/CS nanocomposite.

3.1.1. Scanning electron microscopy

The surface homogeneity and morphologies of α-Fe$_3$O$_4$/CS nanocomposite and CS electrode have been investigated using scanning electron microscopy (SEM, Fig. 1). Fig 1a shows the SEM of α-Fe$_3$O$_4$ nanoparticles. A net with tiny particles hanging on it, is noticed for α-Fe$_3$O$_4$/CS nanocomposite scan in Fig. 1b, which reveals the embedding and incorporation of the α-Fe$_3$O$_4$ nanoparticles in CS film, indicating the formation of α-Fe$_3$O$_4$/CS nanocomposite. The net shape may be attributed to electrostatic interactions between cationic CS and the surface charged α-Fe$_3$O$_4$ nanoparticles. However, in case of pure CS film, Fig. 1c, the net morphology changes to homogenous, regular form.

This suggests that α-Fe$_3$O$_4$ nanoparticles increases the electroactive surface area of CS by increasing its folds and changing it into net providing a favorable environment for trapping heavy metals inside it. These results are further supported by electrochemical studies.
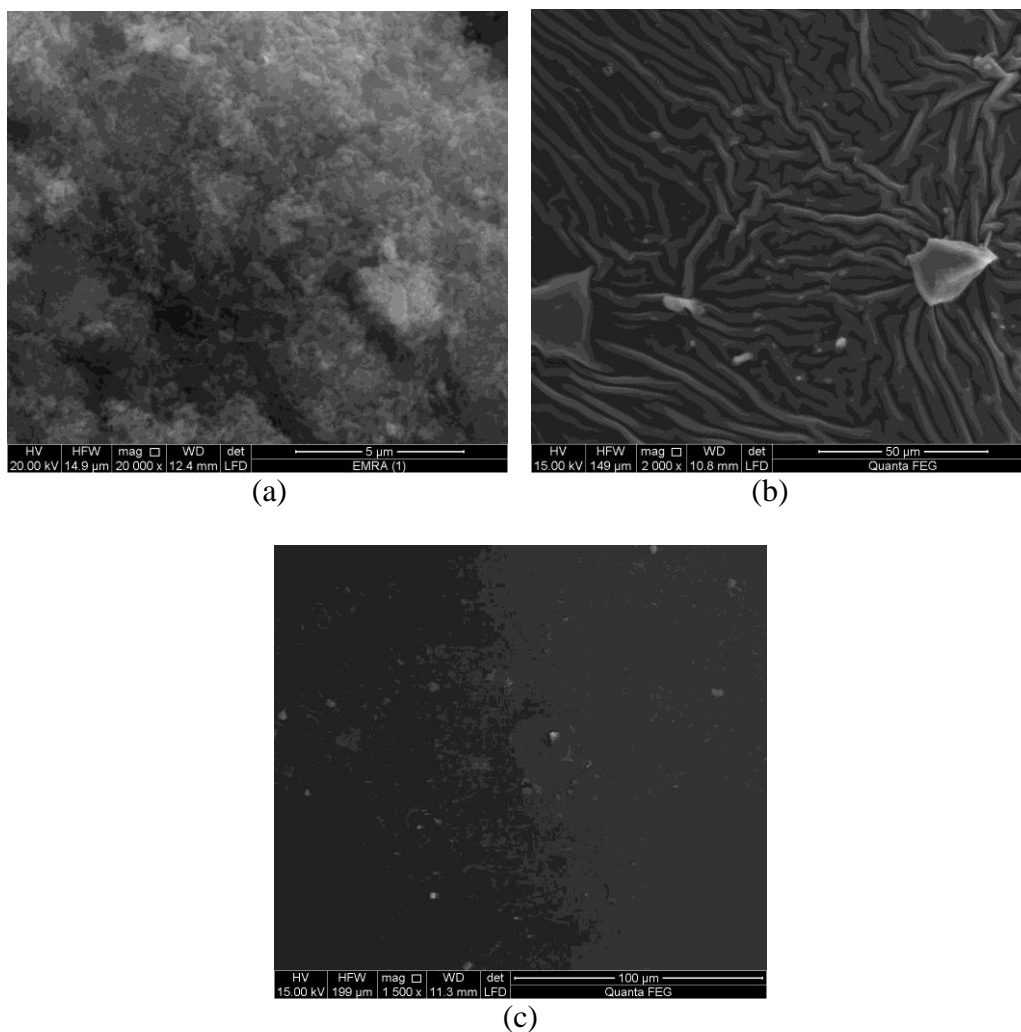

(a)   (b)

(c)

Figure 1. SEM images of (a) α-Fe$_3$O$_4$ nanoparticles, (b) α-Fe$_3$O$_4$ /CS nanocomposite; (c) CS.

3.1.2. Energy Dispersive X-ray analysis (EDX)

The objective of performing EDX analysis on Ni/α-Fe$_3$O$_4$/CS nanocomposite is to investigate the element presence, as it was shown in Fig.2. This analysis was performed with Ni which have good results and high current response determined by α-Fe$_3$O$_4$/CS electrode. As can be seen from this figure the amount of incorporated Fe(III) with respect to chitosan in Ni/α-Fe$_3$O$_4$/CS nanoparticles is 10.29 wt.%. The amount of Ni was 16.94 wt.%, which represent a very good adsorption by the large surface area of paramagnetic Fe$_3$O$_4$, with good stability and high storage of the chitosan layer. EDX spectra showed that Nickel (as an example of the heavy metals) (Fig.2) was adsorbed with high percentage after using CS/Fe$_3$O$_4$ nanocomposite electrode.
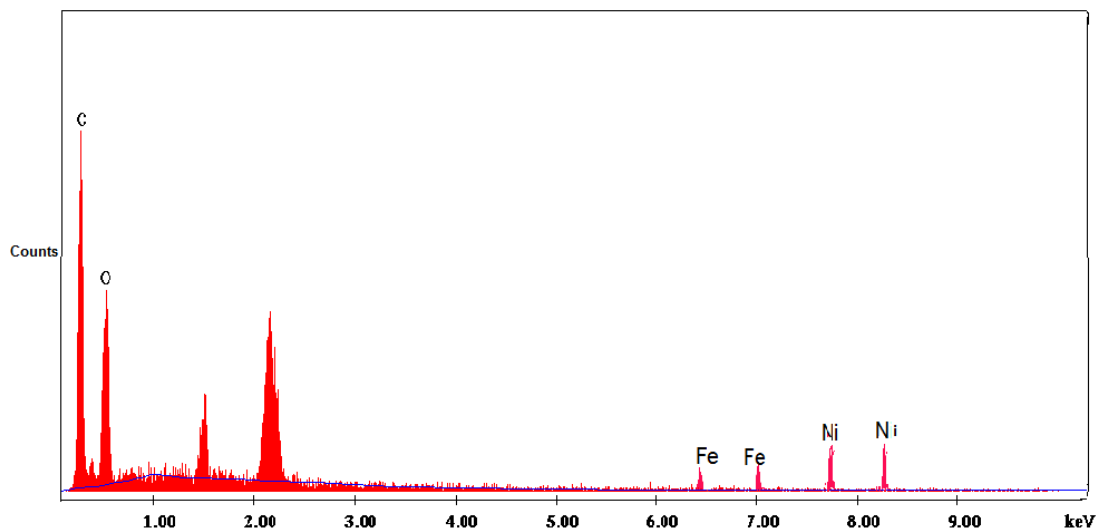
Figure 2. EDX analysis graph for Ni/α-Fe$_3$O$_4$/CS nanocomposite

3.1.3. Thermal gravimetric analysis (TGA)

TGA analysis was performed for chitosan film (a), α-Fe$_3$O$_4$/CS nanocomposite (b), and Ni/α-Fe$_3$O$_4$/CS nanocomposite (c) to estimate the homogeneity and thermal stability of the different films. Fig. 3 (curve a) shows the high thermal stability of chitosan film until 300 ^{o}C losing 25% of its weight.
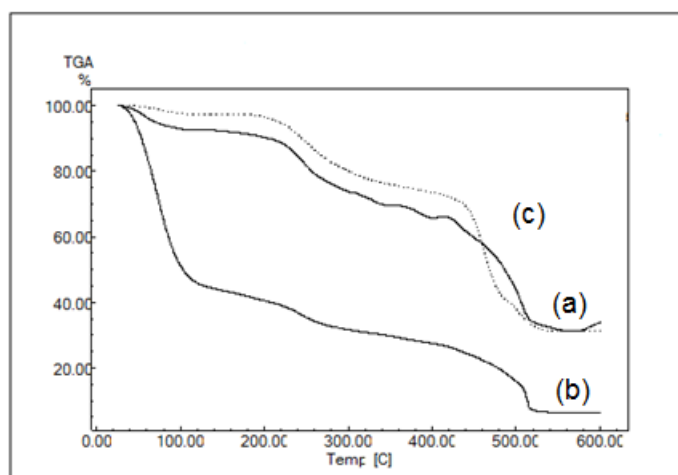

Figure 3. Thermogravimetric analysis for pure chitosan film (a), α-Fe$_3$O$_4$/CS nanocomposite (b), Ni/α-Fe$_3$O$_4$/CS nanocomposite (c).

Meanwhile, it decomposed in three stages starting from 80 ^{o}C. On the other hand, the thermal stability of α-Fe$_3$O$_4$/CS nanocomposite is less stable than pure chitosan film, it decomposes until 300 ^{o}C, and losing 65% of its weight, then it decompose completely at 520 ∘C Fig. 3 (curve b). On the other hand, the thermal stability of Ni/α-Fe$_3$O$_4$/CS nanocomposite Fig. 3 (curve c), which studied after

the absorption of Ni ions inside α-Fe$_3$O$_4$/CS nanocomposite layer, showed higher stability compared to pure chitosan and α-Fe$_3$O$_4$/CS nanocomposite. By comparing the TGA curves at 520 ∘C, where the entire α-Fe$_3$O$_4$/CS nanocomposite was decomposed, however, Ni/α-Fe$_3$O$_4$/CS nanocomposite was still stable. This analysis was repeated three times with the same result, indicating the homogeneity and high stability of the α-Fe$_3$O$_4$/CS nanocomposite after the adsorption of the heavy metals.

3.2. Electrochemical studies

3.2.1. Characterization and voltammetric behavior of the electrode

A peak current response for modified chitosan film by As(III), Pb(II) and/or Ni(II) was performed by CV. Measurements were carried out separately for the analytes 5.0×10^{-4} mol L^{-1} each in 0.05 mol L^{-1} KNO$_3$ solution using an accumulation potential of - 0.6 V applied for 600 s, in a potential range from - 2.0 to 2.0 V vs. calomel reference electrode raised at a scan rate of 50 mV s^{-1}. The α-Fe$_3$O$_4$/CS nanocomposite (a); CS/Pt electrode (b); and bare Pt electrode (c) are all shown in Fig. 4(A, B, C) for As(III), Pb(II) and Ni(II), respectively. It was observed that the α-Fe$_3$O$_4$/CS nanocomposite (curve a) presented a higher analytical signal for detection of the three ions in comparison to CS/Pt, and bare Pt electrodes. This may be due to the induced magnetization of magnetic domains (α-Fe$_3$O$_4$ nanoparticles) on application of electrical field. It appears that the electric field induces alignment of magnetic nanoparticles in a particular direction and facilitates electron flow resulting in an increased value of current [59]. Ni ions show a higher current signal with value of 174 µA more than As and Pb ions with current values of 138.4 µA and 159 µA, respectively. This can be attributed to high electronegativity of Ni, and its affinity to form a stable complex with Fe$_2$O$_3$, leading to an increase of peak current values.

However, the crosslinking of chitosan (curve b) can improve the ion transportation by a mechanism involving pore and membrane diffusion, as recently described [60, 61]. This could be responsible for the enhanced analytical response of the electrode for metallic ions.
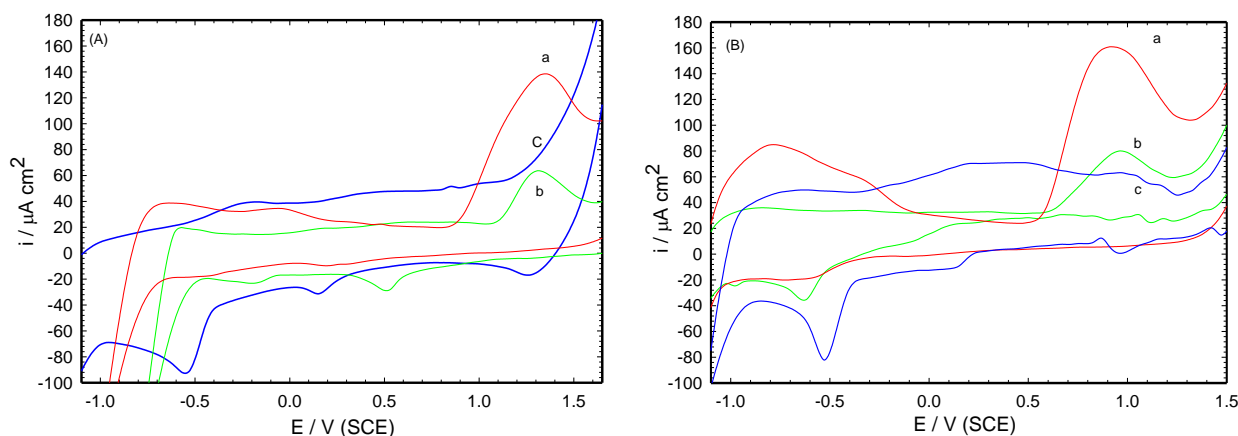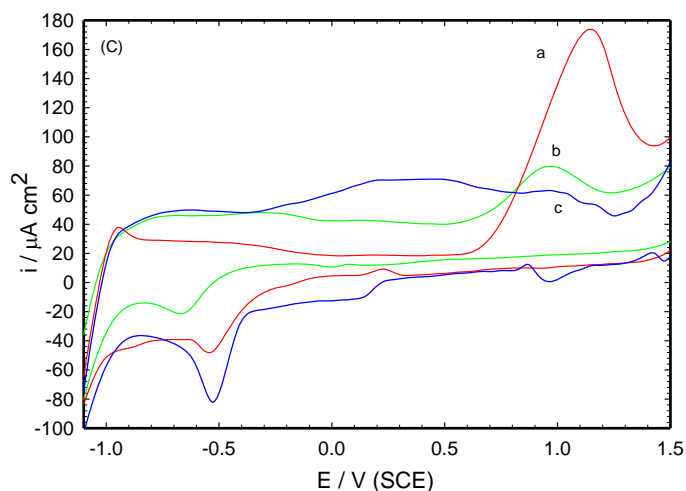
Figure 4. CV of α-Fe$_3$O$_4$/CS nanocomposite (a); CS/Pt electrode (b); and bare Pt electrode (c) in presence of 5.0×10^{-4} mol L^{-1} As(III) (A), Pb(II) (B) and Ni(II) (C).

The crosslinking reactions are usually carried out in order to prevent chitosan dissolution in acidic solutions or to improve the metal adsorption properties, i.e., to increase the capacity or to enhance the selectivity. The presence of hydroxyl group in glutaraldehyde is responsible for metal–chitosan interaction [62]. On the other hand, bare Pt electrode (curve c) has no role in the current enhancement. These results suggest that the presence of Fe$_3$O$_4$ paramagnetic nanoparticles results in an increased electroactive surface area of CS and enhanced electron transfer. Therefore, the α-Fe$_3$O$_4$/CS nanocomposite electrode was selected for further studies owing to the best performance responses for Ni(II), Pb(II) and As(III).

3.2.2. Effect of potential

Figure 5 shows the influence of the accumulation potential on the peak current of As(III) (A), Pb(II) (B) and Ni(II) (C), which was investigated over the potential range from - 1.0 to - 0.2 V.
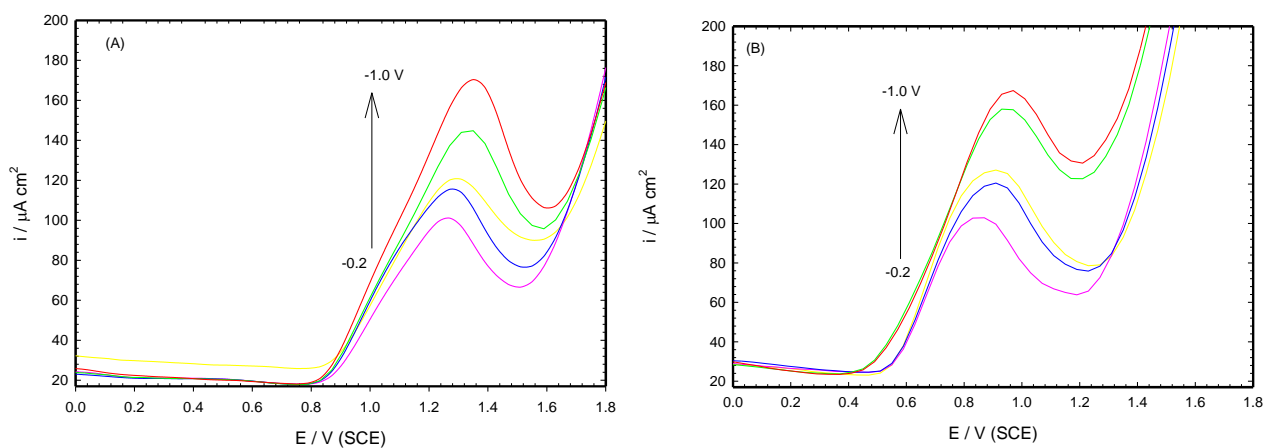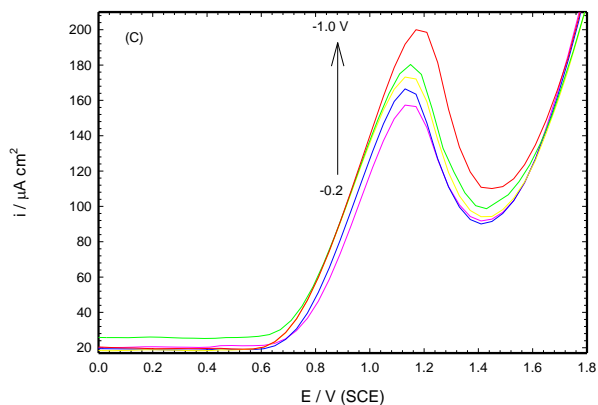
Figure 5. LSV of α-Fe$_3$O$_4$/CS nanocomposite with different potentials in presence of 5.0×10^{-4} mol L^{-1} As(III) (A), Pb(II) (B) and Ni(II) (C).

At more negative potential up to -1.0 V, the ions are reduced more completely, thus the peak current is enhanced greatly. The best definition of the peak current was obtained at a potential of - 0.6 V, achieving a great analytical sharp signal for As(III), Pb(II) and Ni(II) determination with no shift in the peak potential.

3.2.3. Effect of time

The influence of the accumulation time on the anodic peak current for 5.0×10^{-4} mol L^{-1} As(III) (A), Pb(II) (B) and Ni(II) (C) solution using α-Fe$_3$O$_4$/CS nanocomposite electrode is shown in Fig.6. At the same accumulation potential, a longer accumulation time would cause metallic ions to be reduced more completely.
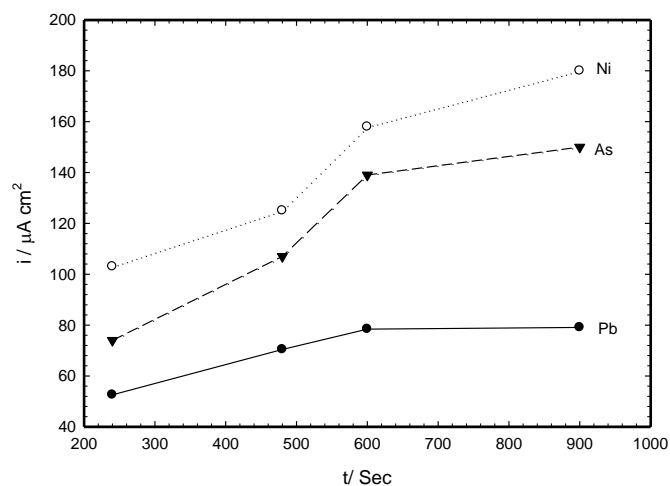

Figure 6. Study of the anodic peak currents obtained by LSV as a function of the accumulation time in the presence of 5.0×10^{-4} mol L^{-1} As(III), Pb(II), and Ni(II). The experimental conditions were 0.05 mol L^{-1} KNO$_3$, accumulation potential of - 0.6V and scan rate of 50 mVs^{-1}

Subsequently, this would lead to a higher peak current. However, when the accumulation time is extremely long the reduced ions covers the entire effective electrode surface, causing saturation for the chitosan layer and hence, the peak current does not change with increasing accumulation time. The maximum peak current were obtained at accumulation time of 600 s for both As and Pb ions. After this time, from 600 to 1000 s, the peak current of the ions remains almost unchanged and the plot becomes almost a straight line, which could be attributed to the fact that the amount of both As and Pb metal ions on the modified electrode surface had greatly increased. However, For Ni ions the current increases continuously as the time increases, as the continuous formation of a complex between Ni and Fe, as mentioned before.

3.2.4. Effect of pH

The effect of the solution pH on the determination of Ni(II) ions from aqueous solution was studied at different pH values (pH 2.0, 5.0, 7.0, 11.0 and 13.0) by recording the oxidation peak of Ni(II) by α-Fe$_3$O$_4$/Cs nanocomposite electrode. Fig. 7 is a plot of oxidation peak currents I$_P$ versus pH of Ni(II), and oxidation peak potentials Ep versus pH, inset. It is clear that the determination process of metal ions was sensitive to pH and usually did not occur at low pH [63]. The results show that by increasing the pH value the peak potential shifted to more positive value. One can see that the oxidation current of Ni(II) ions on α-Fe$_3$O$_4$/CS nanocomposite were increased significantly with the increase of pH value. At low pH (pH < 7), amine groups of chitosan were ionized, the decrease of the adsorption capacities can be attributed to the competitive binding of H$^+$ and Ni(II) ions to amine groups in the composite [64]. Increasing pH to higher values enhanced the adsorption efficiencies for all ions until it reached a maximum at pH 11.0 (figures not shown). The increase of the percent adsorption of Ni(II), by α-Fe$_3$O$_4$/CS nanocomposite at higher pH values could be attributed to the hydrolysis of the metal ions.
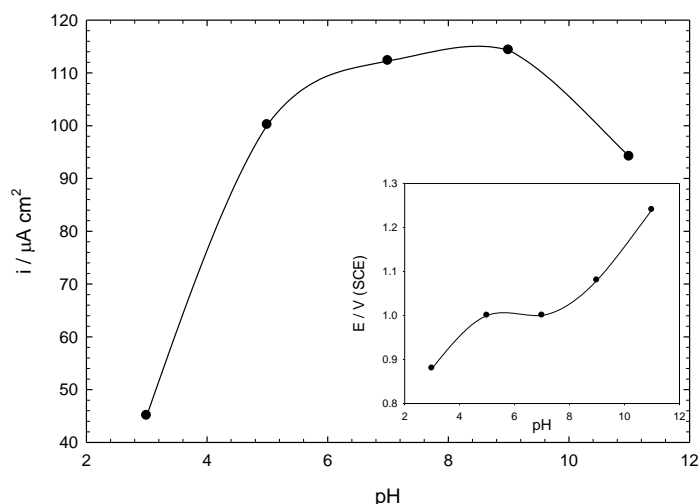

Figure 7. Study of the I$_p$ and E$_p$ (inset) obtained by LSV as a function of pH in the presence of 5.0×10^{-4} mol L^{-1} Ni(II). The experimental conditions were 0.05 mol L^{-1} KNO$_3$ adjusted with 0.05 mol L^{-1} KOH, accumulation potential of - 0.6V for 600 s and scan rate of 50 mVs^{-1}

3.3. Analytical measurement

3.3.1. Calibration curve

The relationship between the anodic peak current and the Ni(II) concentration was also studied. Well-defined peaks were observed by applying an accumulation potential of - 0.6 V for 600 s following the LSV with a scan rate of 50 mV s^{-1} in a concentration range from 5.0×10^{-8} to 1.0×10^{-4} mol L^{-1}. In addition, the calibration curves were observed in Fig. 8. It can be seen that the peak current increased proportionally with the concentration of Ni(II) forming two linear ranges from 5.0×10^{-8} to 1.0×10^{-6} with a correlation coefficient of 0.960 and a detection limit of 3.5×10^{-9} mol L^{-1} and from 3.0×10^{-6} to 1.0×10^{-4} with a correlation coefficient of 0.999 and a detection limit of 4.3×10^{-9} mol L^{-1} ($3 \times$ SD/m, where SD is the standard deviation of blank and m is the slope of the analytical curve). The response characteristics of the proposed method were compared with those reported in the literature with different electrodes developed for Ni(II) (table 1). It can be seen that the proposed α-Fe$_3$O$_4$/CS nanocomposite electrode is simple, low cost, prepared in one step, and finally, has a good detection limit with a low deposition time as compared to most of the other methods for the electrochemical determination of Ni(II).
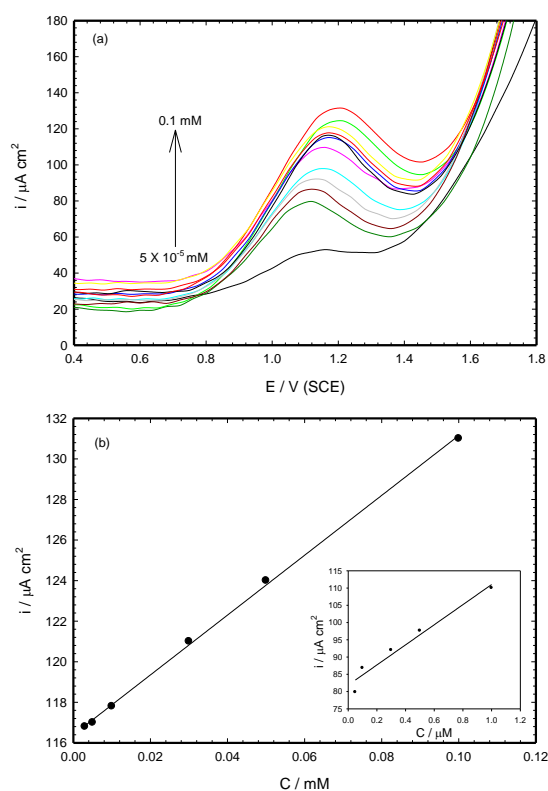
Figure 8. Voltammograms (a) and calibration (b) curve obtained α-Fe$_3$O$_4$/CS nanocomposite electrode in different Ni(II) concentrations in the high linear range from 3.0×10^{-6} to 1.0×10^{-4} and lower linear range from 5.0×10^{-8} to 1.0×10^{-6} (inset) . The experimental conditions were 0.05 mol L^{-1} KNO$_3$, accumulation potential of -0.6V for 600 s and scan rate of 50 mVs^{-1}.

Table 1. The response characteristics of the proposed method compared with those reported in the literature with different electrodes developed for Ni(II)

electrode	Modifier	Method	Deposition time (s) / potential	L.D. (nmol L^{-1})	Refs.
(HMDE)$_a$	DMG, Nioxime	(DPASV)$_b$	60 s, -300mV	-	65
(HMDE)$_a$	Oxine	(DPASV)$_b$	20s, -100 mV	5	66
(HMDE)$_a$	(DMG)$_c$	(SWV)	30 s 120 s,	2 0.2	67
Pt	α-Fe$_3$O$_4$/CS	(LSASV)$_d$	600 s, -600 mV	3.5 4.3	Our work

$_a$ Hanging mercury drop electrode,

$_b$ differential pulse anodic stripping voltammetry,

$_c$ Dimethylglyoxime ,

$_d$ Linear sweep anodic stripping voltammetry .

3.3.2. Application (Real sample analysis)

Table 2. Results obtained with the recovery studies for Ni(II), As(III), and Pb(II) in sewage water and human urine.

Ni(II) concentration (µmol L^{-1})			
Sample	Added	Found	Recovery (%)
Human urine	0.2	0.19	95
	4	3.8	95
	10	9.8	98
sewage water	0.2	0.18	90
	4	3.7	92
	10	9.6	96
As(III) concentration (µmol L^{-1})			
Sample	Added	Found	Recovery (%)
Human urine	0.2	0.18	95
	4	3.7	92
	10	9.9	99
sewage water	0.2	0.19	95
	4	3.7	92
	10	9.9	99
Pb(II) concentration (µmol L^{-1})			
Sample	Added	Found	Recovery (%)
Human urine	0.2	0.18	90
	4	3.7	92
	10	9.9	99
sewage water	0.2	0.18	90
	4	3.9	97
	10	9.8	98

The proposed method was employed in different samples to determine Ni(II), As(III), and Pb(II) in sewage water and human urine samples and verify its potential application. The different samples were spiked with known amount of metal ions standard solution and the total concentration of metal ions was analyzed using the α-Fe$_3$O$_4$/CS nanocomposite electrode. Table 2 summarizes the results obtained with the recovery studies. The mean of the recovery was calculated as the ratio, expressed as a percentage, of the total nickel concentration founded and the nickel concentration added to the samples.

Consequently, the developed α-Fe$_3$O$_4$/CS nanocomposite electrode presented a good accuracy for Ni(II), As(III), and Pb(II) determinations in the samples matrix studies.

3.4. Electrochemical impedance (EIS)

Figure 9 shows EIS scans (Nyquist plots) of CS/Pt, Ni/CS/Pt and Ni/α-Fe$_3$O$_4$/CS nanocomposite electrodes after immersion in the test solution. The impedance value depends on the nature of electrode composition. It is of interest to observe that the arc diameter in Nyquist plot i.e. impedance value, increases in the following order: CS/Pt > Ni/CS/Pt > Ni/α-Fe$_3$O$_4$/CS, which confirms the previous obtained results that Ni/α-Fe$_3$O$_4$/CS electrode is the most efficient one with lowest impedance value. So, modifying CS/Pt electrode by adding α-Fe$_3$O$_4$ to the CS leads to a decrease in coating resistance. This trend is most likely a result of an increase in the surface film capacitance with an increase in the adsorbed amount of Ni ions on the electrode surface.

The impedance data were thus simulated using an appropriate equivalent circuit that gave a reasonable fit with a minimum amount of circuit components. The impedance response of a modified electrode in an aqueous solution is well simulated using a model consists of two circuits from WC$_1$ and RC$_2$ parallel combination (inset in Fig.9) and the two are in series with the solution resistance (R$_s$). By this way C$_1$ is related to combinations from the capacitance of the outer layer and C$_2$ of the inner layer while R is the resistance of the inner layer [68]. Warburg impedance (W) [69] can be linked to ion diffusion through the passive film. This Warburg impedance indicates that the reaction mechanism is controlled not only by a charge-transfer process but also by a diffusion process. Fitting procedures have shown that a good agreement between the theoretical and experimental data (2% error) is obtained. A constant phase element (CPE) is introduced instead of pure capacitor due to frequency dispersion as a result of distribution of relaxation times and inhomogenities, as well as static disorders such as porosity. The impedance (Z$_{CPE}$) described by the expression [68-70]:

$$Z_{CPE} = 1 \Big/ C(j\omega)^{\alpha} \qquad\qquad (1)$$

where $0 \leq \alpha \leq 1$. In this complex formula an empirical exponent (α) varying between 0 and 1, is introduced to account for the deviation from the ideal capacitive behavior due to surface inhomogeneties, roughness factors and adsorption effects [71,72]. In all cases, good conformity between theoretical and experimental was obtained for the whole frequency range with an average error of 4%.

The Stability of best electrode (Ni/α-Fe$_3$O$_4$/CS) nanocomposite was studied with immersion time for 16 h. The experimental values are correlated to the theoretical impedance parameters of the equivalent model given in Table 3. It was found that the film is stable in the range of 16 h. This indicates a better mechanical stability and good adhesion of the Ni, α-Fe$_3$O$_4$ with chitosan.
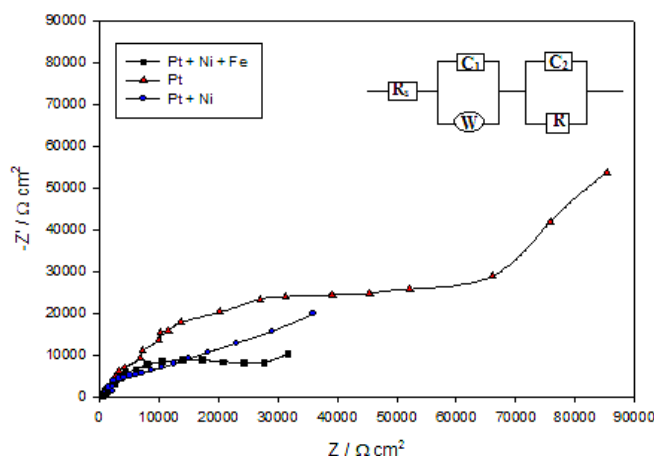

Figure 9. Nyquist plots of α-Fe$_3$O$_4$/CS nanocomposite; CS/Pt electrode and bare Pt electrode in presence of 5.0×10^{-4} mol L^{-1} Ni (II), the model used is inset.

Table 3. Impedance Parameters for Ni (5.0×10^{-4} mol L^{-1}) on α-Fe$_2$O$_3$/CS in 5.0×10^{-4} mol L^{-1} each in 0.05 mol L^{-1} HNO$_3$ solution with immersion time, at 25°C.

Time hour	R_s / Ω cm^2	W / Ω Ω s$^{-1/2}$	C_1 / $\Box$F cm^{-2}	$\Box_\Box$	R / k$\Box$ cm^2	C_2 / $\Box$F cm^{-2}	$\Box_\Box$
0.00	119	5.90	0.95	0.68	29.9	0.36	0.97
0.25	108	8.27	0.73	0.67	43.2	0.35	0.98
0.50	111	9.82	0.67	0.67	64.5	0.32	0.98
1.00	110	11.5	0.54	0.69	91.8	0.31	0.99
2.00	110	12.3	0.43	0.58	124	0.28	0.97
3.00	109	15.7	0.39	0.57	140	0.25	0.98
4.00	111	18.3	0.35	0.57	151	0.23	0.98
8.00	111	23.7	0.25	0.59	165	0.23	0.99
12.00	109	24.5	0.15	0.58	170	0.21	0.98
16.00	108	36.1	0.10	0.57	177	0.20	0.99

4. CONCLUSION

A biosensor has been developed, based on the combination of chitosan crosslinked with glutaraldehyde modified with paramagnetic Fe$_3$O$_4$. The α-Fe$_3$O$_4$/CS nanocomposite film which can be easily prepared exhibits high accumulation ability for the determination and removal of heavy metals

with remarkable current and rapid response. The order of metal ion removal from aqueous solution was Ni (II) > As(II) > Pb(II).

Nanocomposite films were characterized by SEM, EDX, TGA and electrochemical measurement. It is the author's hope that these results will be helpful for researchers who are interested in synthesizing and applying α-Fe$_3$O$_4$/CS nanocomposite electrode as a sensor for determination and removal of heavy metals from aqueous solutions.

References

1. S.E.Bailey, T.J.Olin, R.M.Bricka, D.D.Adrian, *Water Res.* 33(1999) 2469.
2. M.Miro, J.M.Estela, V.Cerda*, Talanta,* 63 (2004) 201.
3. C.Duran, A.Gundogdu, V.N.Bulut, M.Soylak, L.Elci, H.B.Senturk, M.Tufekci, *J. Hazard. Mater.,* 146 (2007) 347.
4. G. Goldstein, A. Asbury, I. Diamond, *Arch. Neurol.* 31 (1974) 382.
5. M.W. Adler, C.H. Adler, *Clin. Pharmacol. Ther.* 22 (1977) 774.
6. I. D_portes, J. L. Benoit-Guyod, D. Zmirou, *Sci. Total Environ.* , 172 (1995) 197.
7. V. Barcan, E. Kovnatsky, *Water Air Soil Pollut.* 103 (1998) 197.
8. N. S. Karam et al., *J. Plant Nutr.* 21 (1998) 725.
9. S. P. McGrath, in Heavy Metals in Soils (Ed: B. J. Alloway), 2nd ed., Blackie Academic and Professional, London (1995) pp. 152 – 174.
10. B. J. Alloway, in Heavy Metal in Soils (Ed: B. J. Alloway), 2nd ed., Blackie Academic and Professional, London (1995) pp. 25 – 34.
11. M. Astrom, A. Bjorklund, *Water Air Soil Pollut.* 89 (1996) 233.
12. J. J. G. Zwolsman, A. J. van Bokhoven, *Water Sci. Technol.* 56(2007) 45.
13. Y. Guo, H. Marschner, *J. Plant Nutr.* 18 (1995) 2691.
14. D. E. Salt et al., Phytoremediation:, *Biotechnol.* 13(1995) 468.
15. Vigo, J. B., and J. T. Ellzey, *Texas J. Microsco.* 37 (2006) 45.
16. M. Kornaros, G. Lyberatos, *J. Hazard. Mater.* 136 (2006) 95.
17. Y. Fu, T. Viraraghavan, *Bioresour Technol.* 79 (2001) 251.
18. J. Gao, Q. Zhang, K. Su, R. Chen, Y. Peng, *J. Hazard. Mater.* 174 (2010) 215.
19. S. Karcher, A. Kornmüller, M. Jekel, *Dyes Pigments* 51(2001) 111.
20. S. Karcher, A. Kornmüller, M. Jekel, *Water Res.* 36 (2002) 4717.
21. M. Wawrzkiewicz, Z. Hubicki, *J.Hazard. Mater.* 164 (2009) 502.
22. M. Wawrzkiewicz, Z. Hubicki, *Chem. Eng. J.* 157 (2010) 29.
23. E. Margui, C. Fontas, M. Hidalgo, I. Queralt, *Spectroc. Acta Part B – Atom. Spectr.* 63(2008) 1329.
24. M. Iqbal, A. Saeed, S.I. Zafar, Hybrid biosorbent: *J. Hazard. Mater.* 148(2007) 47.
25. S.A. Reddy, K.J. Reddy, S. Lakshminaraya, D.L. Priya, Y.S. Rao, A.V. Reddy, *J. Hazard. Mater.* 152(2008) 903.
26. S. Velanki, S. Kelly, T. Thundat, D.A. Blake, H.F. Ji, *Ultramicroscopy* 107(2007) 1123.
27. N. Wang, X.D. Dong, *Anal. Lett.* 41(2008) 1267.
28. H. Xu, L.P. Zeng, S.J. Xing, Y.Z. Xian, G.Y. Shi, *Electroanalysis* 20(2008) 2655.

29. H.C. Yi, P. Mei, *J. Appl. Electrochem*. 38(2008) 1623.
30. Z.W. Zou, A. Jang, E. MacKnight, P.M. Wu, J. Do, P.L. Bishop, C.H. Ahn, *Sens. Actuator B – Chem.* 134(2008) 18.
31. L.H. Marcolino Jr., B.C. Janegitz, B.C. Lourenç, O. Fatibello-Filho, *Anal. Lett*. 40 (2007) 3119.
32. B.C. Janegitz, L.H. Marcolino, O. Fatibello-Filho, *Quim. Nova* 30(2007) 1673.
33. S. Bautista-Banos, A.N. Hernandez-Lauzardo, M.G. Velazquez-del Valle, M.Hernandez-Lopez, E. Ait Barka, E. Bosquez-Molina, C.L. Wilson, *Crop Protection* 25(2006) 108.
34. R.S. Juang, H.J. Shao, *Water Res.* 36(2002) 2999.
35. K. Kurita, *Mar. Biotechnol*. 8(2006) 203.
36. J. Nunthanid, S. Puttipipatkhachorn, K. Yamamoto, G.E. Peck, *Drug Dev. Ind.Pharm*. 27(2001) 143.
37. H.L. Vasconcelos, T.P. Camargo, N.S. Goncalves, A. Neves, M.C.M. Laranjeira, V.T. Favere, *React. Funct. Polym*. 68(2008) 572.
38. H.M. Yi, L.Q. Wu, W.E. Bentley, R. Ghodssi, G.W. Rubloff, J.N. Culver, G.F. Payne, *Biomacromolecules* 6(2005) 2881.
39. S. Sun, A. Wang, *J. Hazard. Mater*. 131(2006) 103.
40. S.T. Lee, F.L. Mi, Y.J. Shen, S.S. Shyu, *Polymer* 42(2001) 1879.
41. C.A. Rodrigues, M.C.M. Laranjeira, V.T. de Favere, E. Stadler, *Polymer* 39 (1998) 5121.
42. K. Inoue, K. Yoshizuka, K. Ohto, *Anal. Chim. Acta* 388(1999) 209.
43. B.C. Janegitz, L.H. Marcolino Jr., S.P. Campana-Filho, R.C. Faria, O. Fatibello-Filho, *Sens. Actuator B – Chem*., 142(2009) 260.
44. R. Pauliukaite, M.E. Ghica, O. Fatibello, C.M.A. Brett, *Anal. Chem.* 81(2009) 5364.
45. L.M. Rossi, A.D. Quach, Z. Rosenzweig, *Anal. Bioanal. Chem*. 380(2004) 606.
46. G.K. Kouassi, J. Irudayaraj, G. McCarty, *J. Nanobiotech*. 3(2005) 1.
47. H. Wei, E. Wang, *Anal. Chem*. 80(2008) 225.
48. S.P. Singh, S. Arya, P. Pandey, B.D. Malhotra, S. Saha, K. Sreenivas, V. Gupta, *App. Phys. Lett*. 91(2007) 63901.
49. A. Wei, X.W. Sun, J.X. Wang, Y. Lei, X.P. Cai, C.M. Li, Z.L. Dong, W. Huang, *App. Phys. Lett*. 89(2006) 123902.
50. A.A. Ansari, A. Kaushik, P.R. Solanki, B.D. Malhotra, *Electrochem. Commun*. 10(2008) 1246.
51. A.A. Ansari, P.R. Solanki, B.D. Malhotra, *Appl. Phys. Lett*. 92(2008) 263901.
52. A. Kaushik, R. Khan, P.R. Solanki, P. Pandey, J. Alam, S. Ahmad, B.D. Malhotra, *Biosens. Bioelectron.* 24(2008) 676.
53. Y.Y. Liang, L.M. Zhang, W. Li, R.F. Chen, *Colloid. Polym. Science* 285(2007) 1193.
54. S.F.Wang, Y.M. Tan, *Analytical Bioanal. Chem*. 387(2007) 703.
55. G. Zhao, J.-J. Xu, H.-Y. Chen, Fabrication, *Electrochem. Commun*. 8(2006) 148.
56. M.S. Lin, H.J. Leu, *Electroanal*. 17(2005) 2068.
57. J. Hrbac, V. Halouzka, R. Zboril, K. Papadopoulos, T. Triantis, *Electroana*. 19(2007) 1850.
58. H.L. Zhang, X.Z. Zou, G.S. Lai, D.Y. Han, F. Wang, *Electroanal*. 19(2007) 1869.
59. A. Kaushik, P.R. Solanki, A.A. Ansari, S. Ahmad, B.D. Malhotra, *Electrochem. Commun*. 10(2008) 1364.
60. J. Cruz, M. Kawasaki, W. Gorski, *Anal. Chem*. 72(2000) 680.
61. M.G. Zhang, C. Mullens, W. Gorski, *Analy. Chem*. 79(2007) 2446.
62. K. Inoue, Y. Baba, K. Yoshizuka, *Bull. Chem. Soc. Jpn*. 66(1993) 2915.
63. S. L. Sun, A.Q. Wang, *Sep. Purif. Technol*. 49(2006) 197.
64. F. A. Alakhras, D.K. Abu, M.S. Mubarak, *J. Appl. Polym. Sci.* 97(2005) 691.
65. H. G. jayarathna , *Current Separation* 19(2001) 77.
66. E. P. Achterberg, C. Braungardt, *Anal. Chim. Acta* 400(1999)381.
67. M. Korolczuk, *Talanta* 53(2000) 679.
68. E. Patrito, V. Macagno, *Electroanal. Chem*. (1994) 375.

69. A. M. Fekry, A.A. Gasser, M.A. Ameer, *Appl. Electrochem.* 4(2010) 739.
70. A. M. Fekry, *Electrochimica Acta.* 54(2009) 3480.
71. F. El-Taib Heakal, A.M. Fekry, A.A. Ghoneim, *Corros. Sci.* 50(2008) 1618.
72. M.J. Esplandiu, E.M. Patrito, V.A. Macagno, *Electrochimica Acta* 40(1995) 809.